ZESZYTY ENERGETYCZNE
TOM IV. *Modelowanie procesów cieplno-przepływowych*
2017, s. 1–12

Pressure drop and temperature uniformity during flow boiling of refrigerant R245fa in microchannels

Stanisława Sandler, Bartosz Zajączkowski, Bogusław Białko

Technical University of Science and Technology, Faculty of Mechanical and Power Engineering
Department of Thermodynamics, Theory of Machines and Thermal Systems
E-mail: stanislawa.sandler@pwr.edu.pl

RECOMMENDATION: *prof. dr hab. inż. Zbigniew Królicki*

ABSTRACT

Cooling computer processors (CPUs) requires dissipating heat from small heat transfer areas. This results in high heat flux densities to be rejected from the microprocessor. Flow boiling in microchannels receives much attention as a potential solution for CPU cooling. It is characterized by high heat transfer coefficients and requires less working fluid inventory than air-based solutions.
However, large pressure drop occurs during phase transition. Moreover, CPU cooling system should provide wall temperature uniformity of the cooled component. Heat transfer coefficient, pressure drop and microprocessor wall temperature depend on microchannel geometry, thermophysical properties of refrigerant, and saturation temperature at which the process is held.
This paper focuses on studying pressure drop and temperature uniformity of 40 x 40 mm microchannel evaporator with R245fa as a working fluid. The analysed heat flux density is 80 $\mathrm{kW/m^2}$ and the vapor quality change along the heat exchanger is 0.2. The study covers saturation temperatures ranging from 30 to 70°C and microchannel diameters varying between 0.35 and 2 mm. Results of the analysis show that the heat transfer coefficient and wall temperature uniformity increase with increasing saturation temperature and decreasing hydraulic diameter. The maximum and minimum observed non-uniformities were 2.58 and 0.69 K, repsectively. Decreasing hydraulic diameter increases pressure losses in the micro-evaporator. The observed pressure drop ranged from 38 to 3753 Pa. Saturation temperature has negligible impact on pressure drop.

KEYWORDS: *flow boiling, microchannel, refrigerant*

1. INTRODUCTION

Progressing miniaturization of computer chips and an increase of their computing power rise cooling demand of microprocessors. For example, the Intel® Core™ i7 processor has a maximum cooling demand of 130 W which is dissipated by the integrated heat spreader (IHS) with the size of ca. 40 x 40 mm [1]. This yields a heat flux density of about 80 $\mathrm{kW/m^2}$. Additionally, the temperature of the processor core (die) should be kept uniform across its surface and not exceed 85°C [4]. A typical processor package assembly is depicted in Fig. 1.

ProcessorAssembly

Fig. 1: Typical processor package assembly: A - IHS, B - die, C - substrate

Cooling requirements can be acheived by micro-evaporators. These heat exchangers consist of parallel coupled microchannels where flow boiling of refrigerant occurs. Details on microchannel cooling can be found in [2].
One of the most commonly used definitions of microchannel has been proposed by Kew and Cornwell [3]. They defined it as a channel with the Confinement number Co lower than 0.5:

$$Co = \frac{[\sigma/(g(\rho_l - \rho_v))]^{0.5}}{d_h} < 0.5 \tag{1}$$

where σ is the surface tension in $\mathrm{N/m^2}$, g is the gravitational acceleration in $\mathrm{m/s^2}$, ρ_l is the density of the liquid phase in $\mathrm{kg/m^3}$, ρ_v is the vapor density in $\mathrm{kg/m^3}$ and d_h is the hydraulic diameter of the microchannel in m.

High values of heat transfer coefficient during flow boiling allow reduction of refrigerant inventory required to cover the cooling demand. Choosing the right refrigerant influences heat transfer rates, pressure losses and system design. The ideal refrigerant should:

- Boil at temperatures lower than the temperature of the cooled component and higher than the temperature of the ambient. The boiling temperature should correspond to the pressure close to the ambient pressure.
- Yield low pressure losses and high heat transfer rates.
- Yield high values of critical heat flux and critical mass flux.
  Under critical heat flux conditions the heat transfer coefficient falls due to formation of a vapor clot at the microchannel wall. This causes an undesired raise in microchannel wall temperature. Refrigerant mass flux equal to or higher than critical mass flux results in occurence of undesired compressible flow effects.
- Be resistant to flow instabilities (such as temperature/pressure oscillations or vapor backflow to the inlet plenum of the heat exchanger).

Saenen [5] conducted an analysis covering 39 refrigerants and concluded that R245fa is a good trade-off for an effective operation of flow-boiling-based cooling system. Agostini et al. [6] and Bertsch et al. [7] pointed out that thanks to its non-flammability and low saturation pressure, R-245fa allows lighter equipment and easier servicing of microelectronics cooling systems. Therefore, this refrigerant has been chosen as a working fluid

for the current analysis. Using Eq. (1), the threshold for transition to microchannel flow boiling for R245fa as a function of saturation temperature has been plotted in Fig. 2.

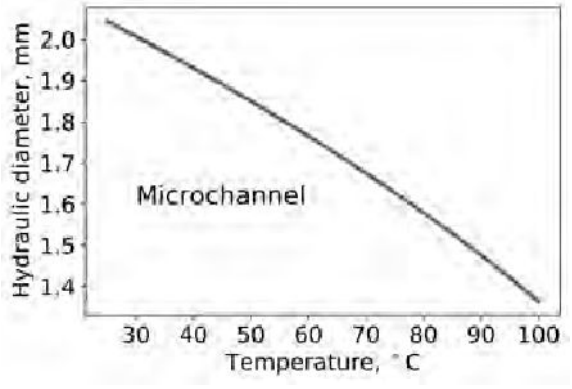

Fig. 2: Threshold for transition to microchannel flow boiling for R245fa

Works studying the behavior of heat transfer coefficient (HTC) of R245fa in micro heat exchangers present changes of HTC with respect to vapor quality x defined as:

$$x = \frac{h - h_l}{h_{lv}} \tag{2}$$

where h and h_l are the enthalpies of the mixture and saturated liquid in $\mathrm{kJ/kg}$, h_{lv} is the latent heat of vaporization in $\mathrm{kJ/kg}$.

Due to imposed heat flux, vapor quality increases along the microchannel length. Studying HTC characteristics as a function of x allows prediction of microchannel wall temperature, which is crucial to design of cooling systems capable of providing safe operating temperature of the die.

The heat transfer coefficient is a function of heat flux supplied, refrigerant mass flux, saturation temperature and resulting refrigerant thermophysical properties as well as channel geometry including surface roughness. However, data presented in the literature shows contradictory trends in HTC behaviour. Some authors reported that HTC falls with increasing vapor quality in the low quality region and rises in the high quality region [8], [10]. Others observed gradual decrease of HTC over the entire range of vapor qualities [9], [11]. HTC exhibits also a non-consistent behaviour with respect to increasing heat and mass flux densities - q, G. Most results of experimental studies show that HTC increases with rising q. Ong and Thome [8] stated that q has little influenece on HTC value, and Agostini et al. [6] reported that its raise causes HTC to decrease at high heat flux densities. In terms of increasing mass flux density G, data shows that it has no effect on HTC [7], causes HTC to go up [8], [6] or fall [11]. The observed discrepancies in data available in the literature may be attributed to non-identical experimental conditions and test stands design. However, further scientific effort is required to fully clarify the inconsistency of the observed trends. Details of experimental studies on flow boiling of R245fa in mini/microchannels together with conditions of the experiments are summarized in Table 1.

The inconsistency of the observed behavior of HTC with respect to vapor quality makes it difficult to develop theoretical models that would be reliable in a wide range of operating conditions. The most recognized models are those of Thome et al. [12] and Bertsch et al. [13]. The first model is based on a two-phase flow pattern. Increas-

ing vapor quality along microchannel length is accompanied by changing flow pattern of the vapor-liquid mixture. When x is low, vapor bubbles are dispersed in the liquid phase (bubbly flow). At moderate x values, bubbles coalescence and form vapor slugs (intermittent flow). At high x values, vapor flows in the central part of the channel and the liquid phase forms a thin annular boundary layer (annular flow).

Thome et al. [12] based their model on the intermittent flow pattern. They assumed that the flow consists of an elongated vapor bubble that is trapped between vapor and liquid slugs (see Fig. 3).

They calculated local mean heat transfer coefficient as a sum of heat transfer through liquid and vapor slugs and a thin film of liquid trapped between the elongated bubble and the microchannel wall. Their model requires initial and minimum values of liquid film thickness as well as a bubble departure frequency.

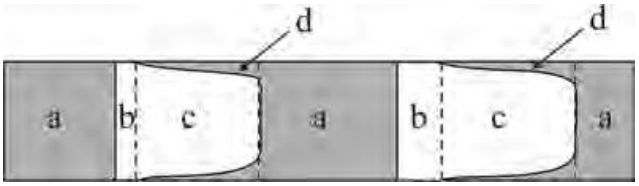

Fig. 3: Flow pattern used in the model by Thome et al. [12]: a - liquid slug, b - vapor slug, c - elongated bubble, d - thin liquid film

Bertsch et al. [13] proposed a model where the heat transfer coefficient is a sum of the nucleate boiling term and the convective term. The first term accounts for heat transfer enhancement due to turbulization of the near wall liquid layer caused by the vapor bubble detachment. The second term addresses heat transfer growth due to forced flow of the liquid-vapor mixture. As vapor quality increases along the microchannel, the thickness of the liquid layer adjacent to the microchannel wall decreases together with the available wall superheat, and the nucleate boiling mechanism is suppressed. At the same time, rising vapor quality result in decreasing density and increasing velocity of the mixture which promotes the convective mechanism. To address these phenomena, the authors introduced correction factors which are functions of vapor quality.

Thermal model used in this article is the one of Bertsch et al. [13] because it can be used in a wide range of operating conditions, in contrast to the model by Thome et al. [12], which is limited to intermittent flow regime.

The aim of this paper is to study pressure drop and wall temperature distribution in a micro-evaporator used for microprocessor coooling. The working fluid is R245fa. The analysis covers microchannels with a hydraulic diameter ranging from 0.35 to 2 mm and fluid saturation temperatures in the range of 30-70°C. The primary objective of this work is analyze the influence of saturation temperature and microchannel geometry on hydraulic losses and wall temperature uniformity in a micro heat exchanger.

Table 1: Summary of experimental studies on flow boiling of R245fa in mini/microchannels

Source	t_{sat} °C	No. channels	Shape	d_h or $W \times H$ mm	Length mm	q kW/m^2	G kg/m^2/s	x	$HTC(x)$ behaviour
Agostini et al. [6]	25	67	rectangular	0.223 x 0.68	20	36–1900	281–1501	0–0.75	For small values of q ($q < 400$ kW/m^2) and $x < 0.1$, HTC increases with increasing x and does not depend on q or G if $G < 1000$ kg/m^2/s. If $G > 1000$ kg/m^2/s, HTC exhibits a U-shaped trend with increasing x. For medium values of q ($400 < q < 1280$ kW/m^2), HTC does not depend on x and increases with rising q or G. For high values of q ($q > 1280$ kW/m^2 at $G = 549.7$ kg/m^2/s and $q > 1375$ kW/m^2 at $G = 690.3$ kg/m^2/s), HTC decreases with rising x or q and increases with rising G.
Bertsch et al. [7]	8–30	17/33	rectangular	0.762 x 1.905	9.53	0–220	20–350	-0.2–0.9	For $x < 0.1$, HTC increases with increasing x. Then it exhibits a plateau. For $x < 0.5$, HTC falls gradually with rising x. HTC rises with increasing q. G does not affect HTC value.
Ong & Thome [8]	31	1	circular	1.03	180	2.3–250	200–1600	0–0.6	For small values of x, HTC remains constant or falls with increasing vapor quality. For higher values of x (transition value of x varied between approx. 0.05 and 0.17 depending on conditions), HTC increases with rising x. HTC showed little dependence on q and increased with increasing G.
Bortolin et al. [9]	31	1	circular	0.96	228.5	5–85	200–400	0.05–0.85	HTC falls with increasing vapor quality and increases with rising q.
Charnay et al. [10]	60–80	1	circular	3	185	10–90	100–1500	0–1.0	HTC remains constant as x or G increases in the low vapor quality region ($x < 0.15 \div 0.2$) and increases with rising x or G in the high vapor quality region ($x > 0.15 \div 0.2$). HTC grows with increasing q or T_{evap}.
Charnay et al. [11]	100–120	1	circular	3	185	10–50	100–1500	0–1.0	HTC increases with increasing q or T_{evap}. At 100°C, HTC falls with increasing x or rising G in the low quality region ($x < 0.2$). HTC remains constant with increasing x and rises with increasing G in the high quality region ($0.2 < x < 0.9$). At 120°C, HTC decreases with increasing x or rising G in the entire range of vapor qualities.

2. PROBLEM DEFINITION

The micro-evaporator analyzed in this study is intended for microprocessor cooling. It is 40 mm long and 40 mm wide. Heat load to be removed from the system Q is 130 W, which using Eq. (3) yields base heat flux density q of 80 $\mathrm{kW/m^2}$.

$$q = \frac{Q}{W \cdot L} \tag{3}$$

where W and L are the width and the length of the heat exchanger base in m.

Working fluid enters the heat exchanger in a saturated state (at $z = 0\ x = 0$). Vapor quality is equal to 0.2 at the outlet due to small size of the heat exchanger. Total mass flow rate of refrigerant $\dot{m}$ is calculated as:

$$\dot{m} = \frac{Q}{\Delta x h_{lv}} \tag{4}$$

where Δx is the change of vapor quality along the heat exchanger.

The heat exchanger consists of N parallel coupled microchannels with rectangular cross section, and the aspect ratio AR is 2. The analysis covers microchannels with hydraulic diameters d_h ranging from 0.35 to 2 mm. Microchannel width a and height b are calculated as follows:

$$a = \frac{d_h \cdot (a + AR)}{2 \cdot AR} \tag{5}$$

$$b = a \cdot AR \tag{6}$$

Equation (5) was taken from [15].

The width of fins that separate microchannels from each other is equal to the microchannel width. Number of channels is calculated with the following formula:

$$N = \frac{W - a}{2 \cdot a} \tag{7}$$

Mass flux density G in a given microchannel is the determined as:

$$G = \frac{\dot{m}}{N \cdot a \cdot b} \tag{8}$$

2.1. Calculation procedure

The calculation procedure involves dividing the heat exchanger into N calculation elements (nicrochannels) having the length of L (see Fig. 4). Each microchannel is divided into n elements with $n + 1$ calculation nodes along its length. We have chosen the grid size $n = 101$. At i-th node vapor quality is calculated as:

$$x_i = \frac{Q}{N \cdot G \cdot h_{lv}} \cdot \frac{i \cdot l_i}{L} \tag{9}$$

where l_i is the length of the i-th element, $l_i = L/n$.

The heat transfer coefficient is determined following the procedure presented in section 3.1. Microchannel wall temperature at each calculation node is then calculated as:

$$t_{w,i} = t_{sat,i} + \frac{q_w}{HTC_i} \tag{10}$$

Pressure drop occuring along each element is calculated using the procedure described in Section 3.2.

Thermophysical properties of R245fa are assumed to be constant across each calculation element, and they are calculated using the CoolProp library [16].

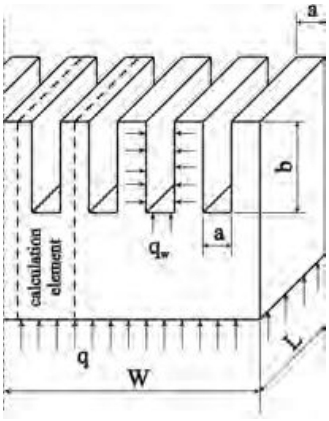

Fig. 4: Calculation domain geometry

3. Mathematical model

3.1. Thermal modeling

In the model by Bertsch et al. [13], the heat transfer coefficient HTC at given vapor quality x equals the sum of the nucleate boiling term and the convective term:

$$HTC = HTC_{nucl} \cdot S + HTC_{conv,tp} \cdot F \tag{11}$$

The nucleate boiling term HTC_{nucl} is given by:

$$HTC_{nucl} = 55 \cdot p_r^{0.12-0.2log_{10}R_p} \cdot (-log_{10}p_r)^{-0.55} \cdot M^{-0.5} \cdot (q_w)^{0.67} \tag{12}$$

where p_r is the reduced pressure, R_p is the surface roughness, if unknown $R_p = 1$, M is the molecular mass of the fluid in $\mathrm{kg/kmol}$, q_w is the heat flux density at the microchannel wall in $\mathrm{W/m^2}$.

The convective term HTC_{conv} can be calculated as a sum of heat transfer coefficients of liquid and vapor phases — $HTC_{conv,l}$ and $HTC_{conv,v}$, respectively:

$$HTC_{conv,tp} = HTC_{conv,l} \cdot (1 - x) + HTC_{conv,v} \cdot x \tag{13}$$

The authors of the model used the Hausen correlation for developing laminar flow [14] to calculate $HTC_{conv,l}$ and $HTC_{conv,v}$ as this is the typical flow regime encountered in microchannels. The correction factors S and F are formulated as folllows:

$$S = 1 - x \tag{14}$$

$$F = 1 + 80 \cdot (x^2 - x^6) \cdot e^{-0.6Co} \tag{15}$$

Equation (15) comes from extrapolation of the experimental data amassed by the authors of the model.

3.2. Hydraulic modeling

Pressure drop across the heat exchanger Δp_{tp} is calculated as a sum of accelerational $\Delta p_{tp,a}$, gravitational $\Delta p_{tp,g}$ and frictional $\Delta p_{tp,f}$ pressure drops:

$$\Delta p_{tp} = \Delta p_{tp,a} + \Delta p_{tp,g} + \Delta p_{tp,f} \tag{16}$$

As the microchannels considered in this paper are horizontal, $\Delta p_{tp,g} = 0$.

Methodology used for prediction of accelerational and frictional terms is based on the paper by Kim and Mudawar [15]. Phase change from liquid to vapor results in decreasing density and increasing velocity of the two-phase mixture. Consequently, an accelerational pressure drop occurs, which is expressed as:

$$\Delta p_{tp,a} = \int_0^L G^2 \frac{d}{dz}\left[\frac{x^2}{\alpha \cdot \rho_v} + \frac{(1-x)^2}{(1-\alpha)\cdot \rho_l}\right] dz \tag{17}$$

The void fraction α (fraction of the channel volume that is occupied by the vapor phase) is calculated from the following relation:

$$\alpha = \left[1 + \frac{(1-x)}{x}\left(\frac{\rho_v}{\rho_l}\right)^{2/3}\right]^{-1} \tag{18}$$

The frictional pressure drop is determined as:

$$\Delta p_{tp,f} = \int_0^L G^2 \left[\frac{2 f_l (1-x)^2}{\varrho_l d_h} \cdot \left(1 + \frac{C}{X} + \frac{1}{X^2}\right)\right] dz \tag{19}$$

where X is the Lockhart-Martinelli parameter defined as [15]:

$$X^2 = \frac{f_l (1-x)^2 \rho_v}{f_v x^2 \rho_l} \tag{20}$$

Friction factors for liquid phase f_l and gas phase f_v depend on the Reynolds number of a respective phase. The correction factor C is a function of the Reynolds, Suratman, Weber and Boiling numbers. For a more detailed description of the procedure for calculation of f and C, the reader is referred to the full version of the article by Kim and Mudawar [15]. Integrals in euqations (18) and (20) are approximated employing the rectangle method.

4. RESULTS AND DISCUSSION

The study focuses on an analysis of pressure drop and wall temperature uniformity along the heat exchanger as a function of micro channel hydraulic diameter and saturation temperature of the refrigerant. The temperature uniformity is defined as:

$$\Delta t_w = t_w^{\max} - t_w^{\min} \tag{21}$$

where $t_w^{\max}$ and $t_w^{\min}$ are the maximum and the minimum wall temperatures in $^\circ$C.

Results are presented in Fig. 5 and Fig. 6. The wall temperature uniformity increases with decreasing hydraulic diameter of the microchannel and increasing saturation temperature of the refrigerant. The maximum and the minimum Δt_w were 2.58 and

0.69 K, respectively. Decreasing diameter of the microchannel results in noticeable pressure drop occurring along the heat exchanger. Increasing saturation temperature causes the hydraulic losses to fall slightly, but its impact is negligible compared to microchannel geometry. The maximum and the minimum Δp were 3753 and 38 Pa, respectively.

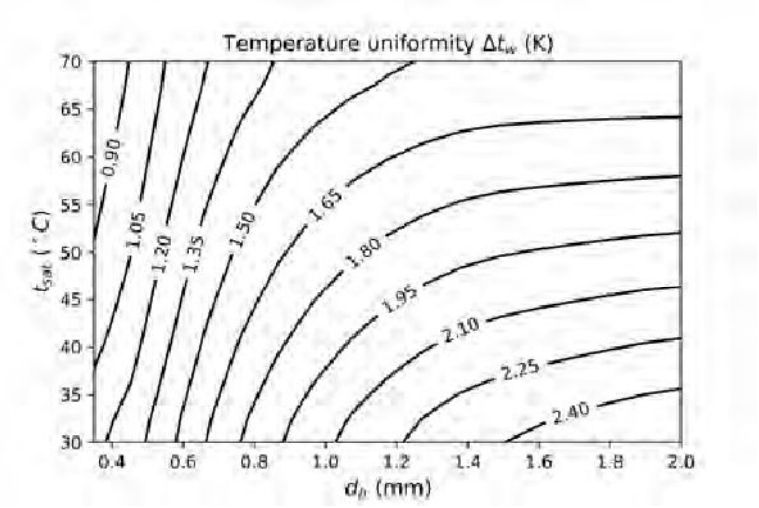

Fig. 5: Wall temperature uniformity as a function of microchannel geometry and refrigerant saturation temperature

Average values of HTC over microchannel length as a function of hydraulic diameter and saturation temperature are plotted in Fig. 7. Distribution of x, HTC, HTC_{nucl} and HTC_{conv} as a function of microchannel length L for chosen values of hydraulic diameter and saturation temperature is presented in Fig. 6.

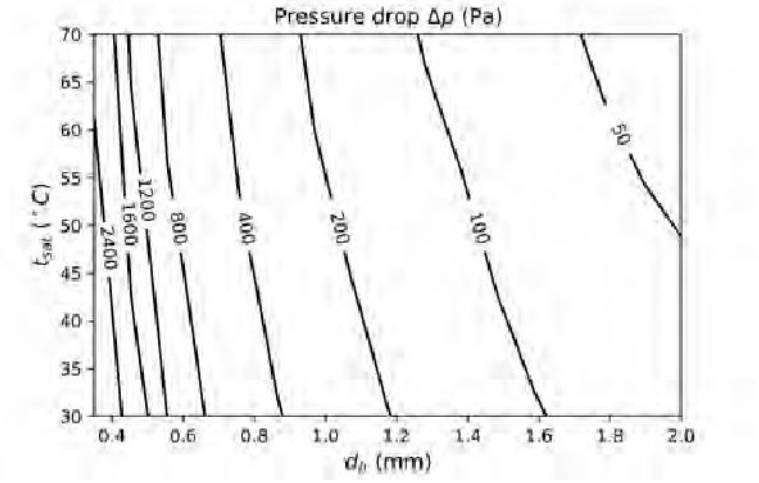

Fig. 6: Pressure drop as a function of microchannel geometry and refrigerant saturation temperature

Distribution of HTC (Fig. 7) shows that its value increases with rising saturation temperature and decreasing hydraulic diameter of the microchannel. These results are consistent with [6], [7], [10], [11] where HTC increases with increasing saturation temperature/pressure. Moreover, Bertsch et al. [7] stated that decreasing hydraulic diameter causes HTC to rise. Comparison of the data with those in Fig. 5 indicates that higher values of HTC promote the uniformity of wall temperature.

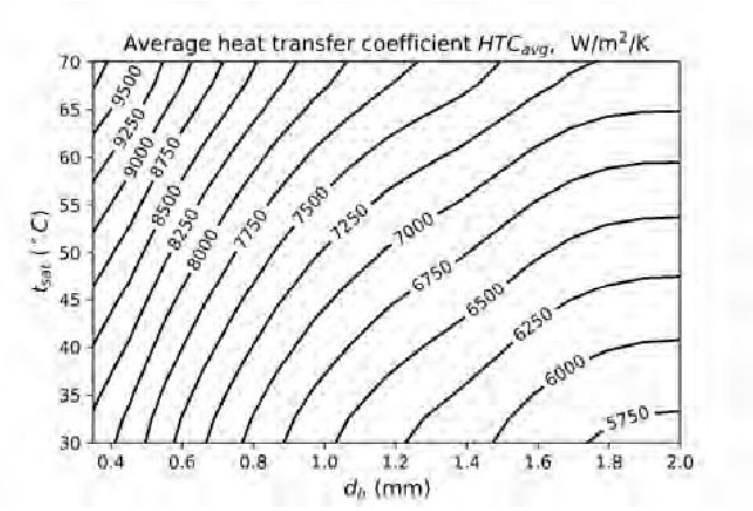

Fig. 7: Heat transfer coefficient as a function of microchannel geometry and refrigerant saturation temperature

Data presented in Fig. 8 shows that HTC and HTC_{conv} decrease slightly for $x < 0.05$ or $x < 0.025$ and considerably increase for higher vapor qualities ($x > 0.05$ or $x > 0.025$) at $d_h = 0.35$ mm and $d_h = 2.00$ mm, respectively. HTC_{nucl} steadily decreases with rising x and microchannel length. At small hydraulic diameters, the convective term dominates over the entire range of the analysed vapor qualities. Increasing hydraulic diameter favors the dominance of nucleate term over the convective one. At $d_h = 2.00$ mm and $t_{sat} = 30°\mathrm{C}$, the nucleate term is higher than the convective one for $x < 0.12$, whereas at $t_{sat} = 70°\mathrm{C}$ for $x < 0.16$. This indicates that increasing saturation temperature favors the nucleate boiling mechanism.

The reason for such behavior is that low hydraulic diameters yield high velocities of the two-phase mixture, which promotes the convective term. At high hydraulic diameters, the convective term dominance is shifted to high vapor quality region. In this region, the density of the mixture decreases due to phase transition, and consequently, the velocity rises. Increasing saturation temperature decreases the required radius of nucleation sites to become active and increases bubble departure frequency [10]. As the number of active nucleation sites and the number of departing bubbles increases, the turbulization of the liquid boundary layer rises, and the nucleate boiling mechanism becomes intensified.

In the range of the analysed conditions similar behavior of $HTC(x)$ was described in [8]. For $q = 78.9\ \mathrm{kW/m^2}$ (which is close to the heat flux density considered in this study $q = 80\ \mathrm{kW/m^2}$) and $G = 400\ \mathrm{kg/m^2s}$, Ong and Thome [8] showed that HTC decreased from 6000 to 5000 $\mathrm{W/m^2K}$ while x changed from 0 to 0.17. Increasing vapor quality from 0.17 to 0.2 caused HTC to rise up to approx. 5500 $\mathrm{W/m^2K}$.

5. Conclusions

This paper presents a study on the impact of microchannel hydraulic diameter and refrigerant saturation temperature on micro heat exchanger operation. Analysed hydraulic diameters and saturation temperatures at the inlet of the heat exchanger ranged from 0.35 to 2.0 mm and 30 to 70°C, respectively. The working fluid was R245fa. The study focused on the assessment of wall temperature uniformity and pressure drop along a micro heat exchanger. Thermal calculations were performed by means of the model proposed by Bertsch et al. [13] and hydraulic calculations employed the approach pro-

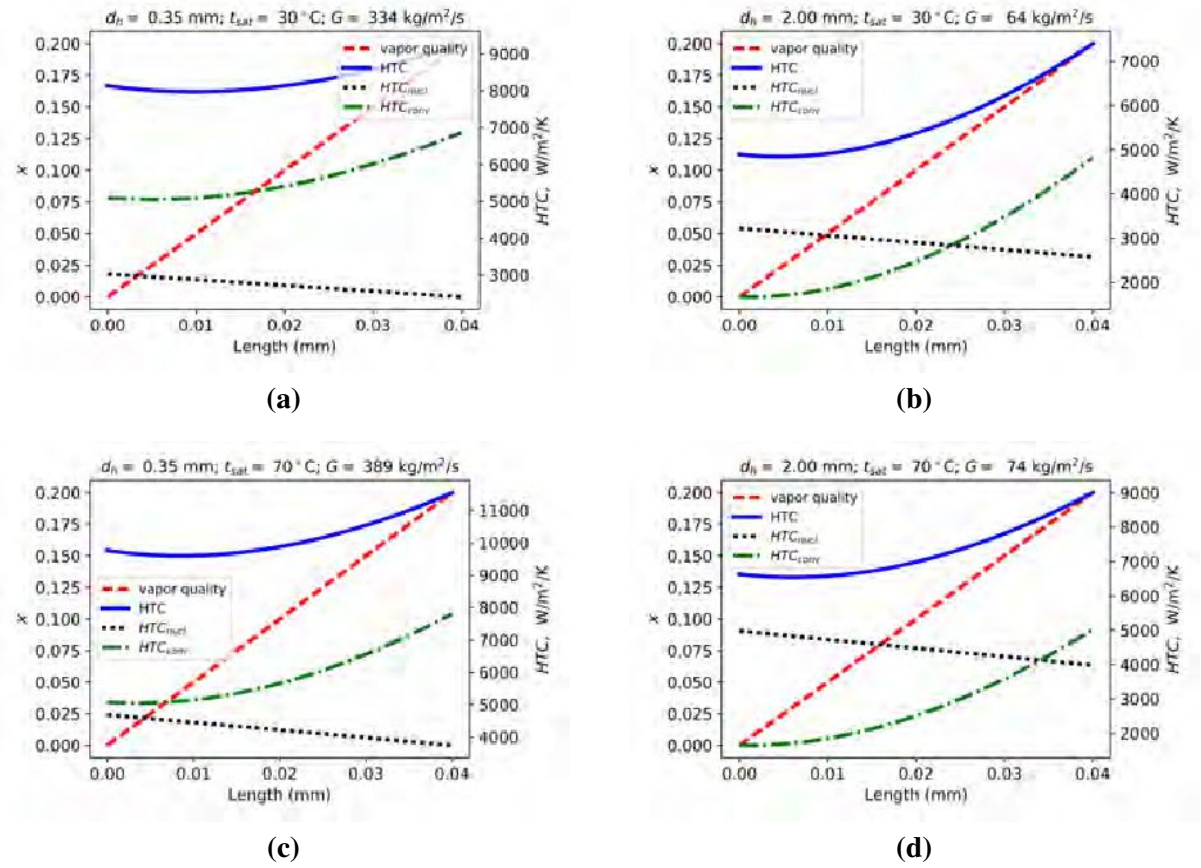

Fig. 8: Heat transfer coefficient and vapor quality as a function of microchannel length (a) $d_h = 0.35$ mm, $t_{sat} = 30°\mathrm{C}$, $G = 334\ \mathrm{kg/m^2s}$ (b) $d_h = 2.00$ mm, $t_{sat} = 30°\mathrm{C}$, $G = 64\ \mathrm{kg/m^2s}$ (c) $d_h = 0.35$ mm, $t_{sat} = 70°\mathrm{C}$, $G = 389\ \mathrm{kg/m^2s}$ (d) $d_h = 2.00$ mm, $t_{sat} = 70°\mathrm{C}$, $G = 74\ \mathrm{kg/m^2s}$

posed by Kim and Mudawar [15]. Results of the analysis showed that in the range of the analysed parameters:

- The difference between maximum and minimum wall temperatures ranged from 0.69 to 2.58 K. Wall temperature uniformity increases with decreasing hydraulic diameter of the microchannel and increasing saturation temperature of the refrigerant.
- The minimum and maximum values of HTC averaged over microchannel length were 5636 and 10140 $\mathrm{W/m^2K}$. Higher values are obtained for high saturation temperatures and small microchannel hydraulic diameters and result in increased uniformity of the wall temperature.
- At low hydraulic diamteres, the prevailing heat transfer mechanism is convective boiling. High hydraulic diameters promote the dominance of nucleate boiling term. The upper limit of vapor quality at which the nucleate boiling term dominates increases with higher saturation temperatures.
- At $d_h = 0.35$ mm and $d_h = 2.00$ mm, the convective term experiences a slight fall for $x < 0.05$ or $x < 0.025$, respectively and considerably increases outside these ranges. HTC_{nucl} steadily decreases with rising x.
- Pressure drop occuring in the heat exchanger ranged from 38 to 3753 Pa. Decreasing microchannel diameter increases the pressure drop. Increasing saturation temperature has a negligible impact on the hydraulic losses.

REFERENCES

[1] *Intel ® Core™ i7-900 Desktop Processor Extreme Edition Series and Intel® Core™ i7-900 Desktop Processor Series*, Datasheet, Vol 1, Intel, February 2010.

[2] Smakulski P., Pietrowicz S., *A review of the capabilities of high heat flux removal by porous materials, microchannels and spray cooling techniques*, Applied Thermal Engineering **104**, 636-646, 2016.

[3] Kew P.A., Cornwell K., *Correlations for the Prediction of Boiling Heat Transfer in Small-Diameter Channels*, Applied Thermal Engineering **17**, 705-715, 1997.

[4] Szczukiewicz S., Borhani N., Thome J.R., *Two-phase flow operational maps for multi-microchannel evaporators*, Int. J. Heat and Fluid Flow **42**, 176-189, 2013.

[5] Saenen T., *Modeling a two-phase microchannel electronics cooling system* (doctoral thesis), Katholieke Universiteit Leuven – Faculty of Engineering, Belgium, 2013.

[6] Agostini B., et al., *High heat flux flow boiling in silicon multi-microchannels – Part II: Heat transfer characteristics of refrigerant R245fa*, Int. J. Heat and Mass Transfer **51**, 5415-5425, 2008.

[7] Bertsch S.S., Groll E.A., Garimella S.V., *Effects of heat flux, mass flux, vapor quality, and saturation temperature on flow boiling heat transfer in microchannels*, Int. J. Multiphase Flow **35**, 142–154, 2009.

[8] Ong C.L., Thome J.R., *Flow boiling heat transfer of R134a, R236fa and R245fa in a horizontal 1.030 mm circular channel*, Experimental Thermal and Fluid Science **33**, 651–663, 2009.

[9] Bortolin S., Del Col D., Rossetto L., *Flow Boiling of R245fa in a Single Circular Microchannel*, Heat Transfer Engineering **32**, 1160–1172, 2011.

[10] Charnay R., Bonjour J., Revellin R., *Flow boiling characteristics of R-245fa in a minichannel at medium saturation temperatures*, Experimental Thermal and Fluid Science **59**, 184–194, 2014.

[11] Charnay R., Bonjour J., Revellin R., *Flow boiling heat transfer in minichannels at high saturation temperatures: Part I – Experimental investigation and analysis of the heat transfer mechanisms*, International Journal of Heat and Mass Transfer **87**, 636–6524, 2015.

[12] Thome J.R., Dupont V., Jacobi A.M., *Heat transfer model for evaporation in microchannels. Part I: presentation of the model*, International Journal of Heat and Mass Transfer **47**, 3375–3385, 2004.

[13] Bertsch S.S., Groll E.A., Garimella S.V., *A composite heat transfer correlation for saturated flow boiling in small channels*, International Journal of Heat and Mass Transfer **52**, 2110–2118, 2009.

[14] Hausen H., *Darstellung des Wärmeüberganges in Rohren durch verallgemeinerte Potenzbeziehungen*, Z. VDI Beiheft Verfahrenstechnik **4**, 91–102, 1943.

[15] Kim SM., Issam Mudawar I., *Review of databases and predictive methods for pressure drop in adiabatic, condensing and boiling mini/microchannel flows*, Int. J. Heat and Mass Transfer **77**, 74–97, 2014.

[16] Bell I.H., Wronski J., Quoilin S., Lemort V., *Pure and Pseudo-pure Fluid Thermophysical Property Evaluation and the Open-Source Thermophysical Property Library CoolProp*, Industrial & Engineering Chemistry Research **53**(6), 2498–2508, 2014.